Title

How deep does an attractive potential have to be to capture n-Ag ?

Author

jayachandran, shwetha

Publication Date

2023

Peer reviewed|Thesis/dissertation

How deep does an attractive potential have to be to capture nAg?

By

SHWETHA JAYACHANDRAN

THESIS

Submitted in partial satisfaction of the requirements for the degree of

MASTER OF SCIENCE

in

Chemical Engineering

in the

OFFICE OF GRADUATE STUDIES

of the

UNIVERSITY OF CALIFORNIA

DAVIS

Approved:

Tonya Kuhl, Chair

Veronica Morales

Scott Bradford

Committee in Charge

2023

Table of Contents

Abstract

The fate of silver nanoparticles (nAg), an emerging environmental contaminant, has been widely studied particularly around wastewater and groundwater systems. The transport and deposition of nanoparticles onto the surface of environmental porous media-like soils are most commonly modeled using classical colloid filtration theory to assess the filtration efficiency and dispersal of suspended nAg in percolating groundwater. However, the variation of porous media including surface roughness and chemical heterogeneity renders findings system specific. This work sought to determine how deep the attractive potential well must be to capture silver nanoparticles (nAg) under conditions where the equilibrium interaction potential should follow classical DLVO modeling. Using a well-defined model system of 50 nm nAg particles and 50 ±10 μm silica collector particles under gravity-driven flow (low Reynolds number and low Peclet number), it was determined that at -2.5 kT attractive well ~ 92 % of nAg were captured in the column. The nAg particles were released by increasing electrostatic repulsion through reduction in ionic strength. Subtle changes in the ionic strength in the range 5 to 12.5 mM, which are commonly found in soil, transitioned from transport to deposition and vice versa. These findings will be useful for predicting transport or capture in more complex systems.

Acknowledgments

First and foremost, I would like to thank my advisor Dr. Tonya Kuhl for her invaluable Mentorship throughout my master's degree. Working in the Kuhl lab has been an incredible experience, and Dr. Kuhl's support, guidance, and words of encouragement helped me in shaping my research. I sincerely thank her for giving me the opportunity to work on this project.

I would like to thank my committee members Prof. Veronica Morales and Prof. Scott Bradford for their support and valuable feedback. I would also like to thank the members of my research group: Tanner Finney, Kevin Gu, and Skye Frank their technical support and for helping me improve my research skills.

Lastly, I would like to extend my gratitude to my cherished family and friends. I would like to thank my parents, Jayachandran and Ponni Jayachandran for their unconditional love and support throughout this journey and for allowing me to pursue my dreams. I am immensely grateful to Antony Leo Joan Balthasar for his unwavering and immaculate support from day one. Big thanks to Ujwala Vedavally, Kavya Somayajula, and Raina Joby for making my stay in Davis enjoyable.

1. Introduction

Because of their antimicrobial and antibacterial properties, silver nanoparticles (nAg) are widely used in various consumer products including textiles, cosmetics (Badawy et al. 2010), medical devices, and drug delivery (Lee and Jun 2019; Cornelis et al. 2013; Badawy et al. 2010). As a result, nAg enters the environment through wastewater effluents (Patiño, Kuhl, and Morales 2020; Cornelis et al. 2013) and can contaminate water sources and soil (Mahdi et al. 2018). To evaluate the risk and toxicity of nAg in the environment, understanding its colloidal deposition, transport, and retention is essential (Cornelis et al. 2013; Godinez et al. 2013). The physiochemical factors that alter nAg transportation are pH, ionic strength (Liu, Sun, and Santamarina 2019; Patiño, Kuhl, and Morales 2020), porous media size distribution (Mahdi et al. 2018), surface roughness (Bradford and Torkzaban 2015), heterogeneous collector surface (Lin et al.2011), and particle flow (Liang et al. 2013). Previous work on the transportation and retention of particles in saturated porous media has varied these physiochemical factors including the concentration of nAg (Liang et al. 2013), particle size, pH,ion type (Liang et al.2013), ionic strength (Mahdi et al. 2018), the role of dissolved organic matter (Sagee, Dror, and Berkowitz 2012), humic acid (Patiño, Kuhl, and Morales 2020), and carbonate absorption (Liu et al. 2019).

Colloidal filtration theory (CFT), presented by Harvey and Garabedian 1991 ES&T, has been used extensively to model the fate of nAg in the environment. CFT combines convection and diffusion of nanoparticles with classical colloidal interactions, and a sink term to predict the retention of nAg in soil (Harvey and Garabedian 1991; Liang et al. 2013; Yao, Habibian, and O'Melia 1971). In the CFT governing equation (Eq. 1), C is the nanoparticle concentration, D is the dispersion coefficient, v is the mean pore velocity, and k_d is the irreversible deposition rate.

The rate constant k_d depends on the attachment efficiency α, media porosity θ, mean particle radius R_M, and single collector efficiency η_0. This approach has been used extensively in the field of environmental remediation to better understand and predict the fate of nAg.

$$\frac{\partial C}{\partial t} = D\frac{\partial^2 C}{\partial x^2} - \upsilon\frac{\partial C}{\partial t} - k_d C \qquad \text{Eq. (1)}$$

$$k_d = \frac{3}{4}\frac{(1-\theta)}{R_M}\upsilon\alpha\eta_0 \qquad \text{Eq. (2)}$$

The specific objective of this research was to quantitatively establish the depth of the attractive well required to capture nAg particles in a well-defined system. The column was composed of 40 µm silica particles, and the experiments were in the diffusive regime (supporting document) with nAg transported in the column by gravity-driven flow. The foundation for predicting colloidal interactions between particles under the measurement conditions is the Derjaguin,, Landau, Vervey and Overbeek (DLVO) theory (Swanton 1995). By varying the solution ionic strength, the interaction potential between nAg and silica particles could be precisely modulated, enabling the attractive well depth to be quantitatively determined. Significantly, the ionic strength range of interest, 5mM to 25mM, for tuning the nanoparticle fate from transport to capture is in accordance with ionic strengths in typical soils.

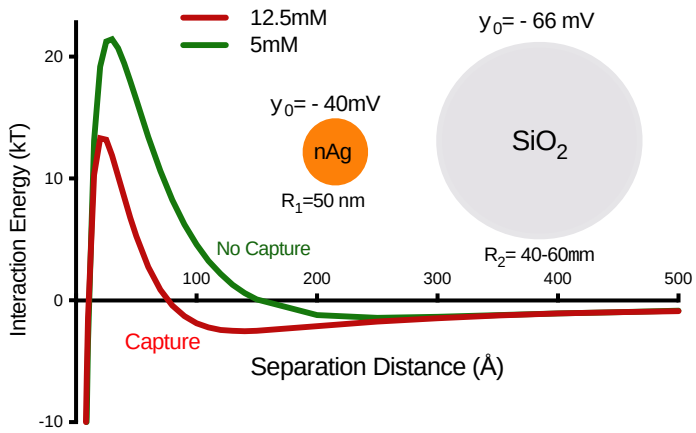

2. Materials and Methods

2.1 Chemicals

Bio Pure monodispersed silver nanospheres with a diameter of 50 nm ± 4 nm,1 mg/ml concentration in 2 mM sodium citrate were purchased from nanocomposix. The sodium citrate coating helps prevent the aggregation of particles and these coatings may affect the surface charge and provide steric and electrostatic repulsion (Petosa et al.2010a) (Sagee, Dror, and Berkowitz 2012). Sodium nitrate ($NaNO_3$,99.995% purity, Sigma) was used to prepare monovalent electrolyte solutions for transport column experiments and zeta potential measurements. Silica gel (Silicon dioxide)230-400 Mesh, Grade 60 was purchased from Fisher Chemical (Thermo Fisher Scientific) with particle sizes 50 ±10 µm. RCA silica beads from polysciences (400nm ± 40nm, $nSiO_2$) were used as a proxy for silica zeta potential measurements. Milli-Q gradient water was used for all experiments.

2.2 Zeta Potential

A Malvern Zetasizer Pro ZS (Malvern Instruments Ltd.) was used to measure the zeta potential of nAg and $nSiO_2$ with different electrolyte solution concentrations. A 1.0 ml sample of

0.01mg/ml concentration of nAg at the desired ionic strength was loaded into DT 1070 disposable folded capillary cells and equilibrated to 25 ºC for 30 seconds. The scattering angle was 90º. Refractive index values for silica and nAg were 1.46 and 0.06, respectively. A minimum of three independent samples were tested with 3 separate measurements of 12 runs each (Table 1). The zeta potential depends on the ionic strength, ion type, and pH but is independent of nanoparticle concentration under these conditions (Liu, Sun, and Santamarina 2019). The pH was not controlled for the measurements to be consistent with column experiments.

Sample	**Particle size (nm)**	**pH**	**Solution**	**Zeta (mV)**
Silica	400 ± 40	8.5	MilliQ	-70 ± 7
Silica	400 ± 40	7.9	10, 12.5mM	-58 ± 8
Silica	400 ± 40	8.1	5, 7.5mM	-74.1±6
nAg	50 ± 4	7.2	MilliQ	-57 ± 10
nAg	50 ± 4	6.1	10, 12.5mM	-39 ± 12
nAg	50 ± 4	6.1	5, 7.5mM	-42 ± 18

Table 1: Zeta potential measurements of silica and nAg as a function of $NaNO_3$ ionic strength. Grouped ionic strengths were indistinguishable from one another.

2.3 Transport column Experiments

Transport and retention of nAg in porous media experiments were carried out in 10 mL polystyrene serological pipettes (1.1 cm inner diameter) from Fisher Scientific. The columns were packed with silica (~1.27 g), these porous media may affect the energy profiles due to charge heterogeneity (Bradford and Torkzaban 2015). To avoid leakage of silica particles from

the column, a cotton plug was placed at the column base prior to filling. The column was then vibrated to achieve uniform packing and to avoid air gaps (Liang et al. 2013). Subsequently, the column was filled with the desired electrolyte solution and flushed at least 5 times. The liquid volume to completely wet the silica was 2 ml, and the residence time for 2 ml was approximately 30 mins. Ionic strengths from 0 to 50 mM $NaNO_3$ were explored. The salt titration data (supplemental information, figure S2) demonstrates that 50nm nAg dispersions were stable below 50 mM ionic strength. Figure 1 shows the column setup under different ionic strengths.

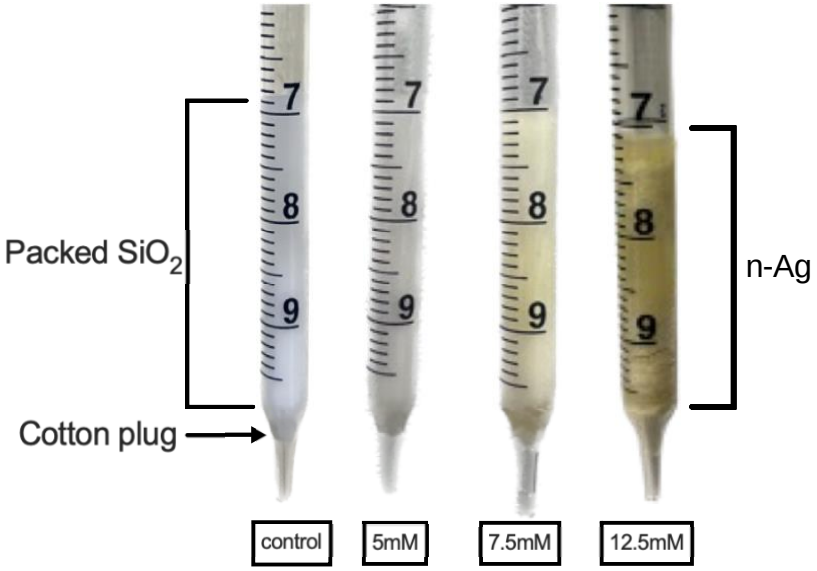

Figure 1. Transport and retention of nAg in the SiO_2 column at different ionic strengths (control, 5mM, 7.5mM, and 12.5mM $NaNO_3$). The control column contains only the background electrolyte solution.

Silver nanoparticle samples at a concentration of 0.05 mg/ml in the desired ionic strength were sonicated before adding to the wetted column at the same ionic strength (Sagee, Dror, and Berkowitz 2012). No pressure was applied, and the silver particle solution moved through the column by gravity-driven flow (natural convection) under creeping flow conditions (Supporting Information). A load volume of 2 ml was used in all cases and flush volumes were also done in 2 ml aliquots. The effluent samples were collected in 250μL fractions in borosilicate glass tubes

for concentration determination using a UV-vis spectrophotometer (Molecular Devices SpectraMax 384 plus Microplate Reader) with a 96-well PCR plate (Thermo Fisher Scientific). A wavelength of 420 nm and path length of 0.5 cm was used to quantify the concentration using Beer Lambert's law. Known concentrations of nAg stock were used to establish an absorption calibration curve (supplemental information, figure S1). In some cases, the silica column was dried and broken down after the experiments to determine whether the particles adhered to the column walls. Adhesion to the walls was not observed. In addition, nAg was found to adsorb to the cotton fibers in the cotton plug. The adsorbed amount was quantified by soaking a cotton plug in different electrolyte solutions with 0.05 mg/ml nAg for approximately 2 hours. After removal of the cotton plug, the absorbance value showed that approximately 16 ± 13.5 % of nanoparticles were absorbed to the cotton plug. At least triplicate experiments were conducted in all cases and the average of these experiments is reported.

2.4 Interaction Energy Profile -DLVO Theory

For nAg in a hydrated, porous silica column, the dominant interactions are van der Waals attraction and electrostatic repulsion. In this well-defined system, DLVO theory can be used to accurately predict the interaction energy between nAg and the much larger silica particles. The electrostatic energy ($V_{elec\ (h)}$) between silica and nAg was calculated using the non-linear Poisson-Boltzmann (NLPB) equation for two flat plates and converted to sphere-sphere interaction using Equation (3) (Grabbe 1993; Patiño, Kuhl, and Morales 2020). For these measurements, the dielectric constant was 78, and temperature 25ºC. The Debye length κ (Å) for monovalent salts was determined from 3.04/√M, where M is molarity. R_1 is the radius of nAg (25 nm), and R_2 is the radius of SiO_2 particles (20 to 30 μm). Since $R_2 \gg R_1$ the interaction is scaled by R_1 of nAg. The surface potential of the nAg and silica was determined by measuring

zeta potential in colloidal suspensions under the relevant electrolyte conditions (Table 1). Equation (4) was used to calculate the van der Waals ($V_{vdW(h)}$) attraction between spheres where D is the separation distance, and A is the Hamaker constant based on the refractive index of silica and Ag, acting in water. The value, $A = 4.3 \times 10^{-20} J$, was used based on experiments by Patiño, Kuhl, and Morales 2020. The total interaction energy between the nAg and the silica particles, $V_T(h)$, is the sum of the van der Waals attraction, ($V_{vdW(h)}$) and electrical double layer interaction, $V_{elec\,(h)}$) (Huynh and Chen 2011).

$$W_{elec} = \left(\frac{R_1 \times R_2}{R_1 + R_2}\right) \times \frac{2\pi}{\kappa} NLPB_{flats} \qquad \text{Eq. (3)}$$

$$W_{vdW} = \frac{-A}{6D}\left(\frac{R_1 \times R_2}{R_1 + R_2}\right) \qquad \text{Eq. (4)}$$

3. Results and Discussion

3.1 Chromatography Column: Transport and Retention

The goal of this work was to experimentally determine the depth of the DLVO attractive well required to capture nAg using a well-defined system with silica collector particles. If the surface roughness of SiO_2 is considered based on the asperities of the sphere on a porous media, then the DLVO calculation should be accounted for sphere and flat plate with alterations in depth of secondary minimum and energy barrier (Shen et al.2012). The size of nanoparticles and porous media could affect the heterogeneity and surface roughness (Petosa et al.2010b). The presence of surface roughness could deepen the secondary minimum well (Shen et al.2012). As the van der Waals attraction is constant, the depth of the minimum can be altered by modulating the electrostatic repulsion through the solution ionic strength (Israelachvili 1991; Israelachvili and Adams 1978; Liang et al. 2013). As shown in Figure 1, the transport or capture of nAg can be qualitatively detected visually at a concentration of 0.05 mg/ml. The control column was filled

with background electrolyte solution (5mM, 7.5mM ,10mM ,12.5mM) The pore volume in a saturated column was 2 ml, and 2 ml aliquots of nAg in the same ionic strength were gently added atop the wetted column at the same ionic strength. The solution was allowed to drain by gravity and an additional 2 ml electrolyte solution only, no nAg, was added atop the wetted column (water saturation) to ensure the column did not dry out. The residence time for 2 ml was approximately 30 mins. By visual inspection and mass balance, at 5 mM ionic strength, the nAg particles eluting from the column was 65 % with 16 ± 13.5 % nAg absorbed in cotton plug. At 7.5 mM and 10 mM the mass recovery was approximately 24 % and 11% respectively with 16 ± 13.5 % nAg absorbed in cotton plug . At 12.5 mM nAg loaded into the column was captured with 8% mass recovery and when re-eluted 41% was the mass recovery (Supporting Information). The attractive minimum was sufficiently deep at 12.5 mM and only clear electrolyte solution eluted.

More quantitative measurements were based on column eluent UV-visible absorbance as shown in Figure 2. At 5 mM the nAg eluted out of the column with ~ 65 % mass recovery. At 12.5 mM the initial eluent was clear. To confirm that the nanoparticles were captured in the secondary minimum and not physically stuck between the collector particles, MilliQ water in 2 ml aliquots was added to reduce the ionic strength and decrease the secondary minimum well depth (Liang et al. 2013). Figure 2(b) demonstrates that the nAg once captured at 12.5mM, eluted when DI was added .The particle remobilization was only tested with DI because it alters the ionic strength and changes the depth of secondary minima and particle stability. Figure 2(c) shows the relevant ionic strength data plotted together for easy comparison.

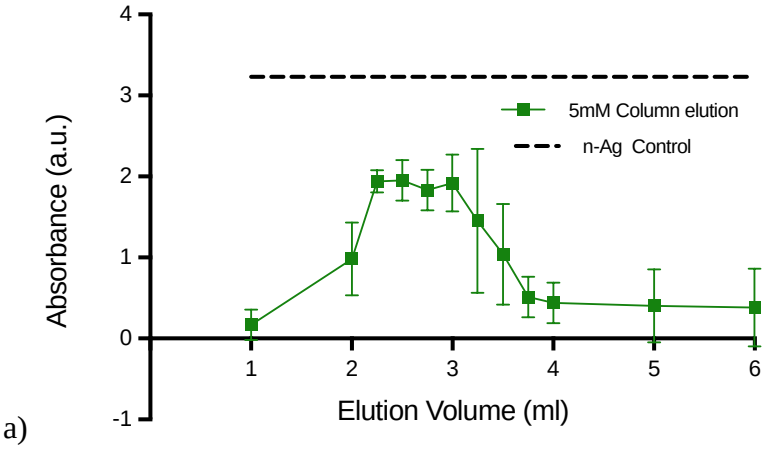

a)

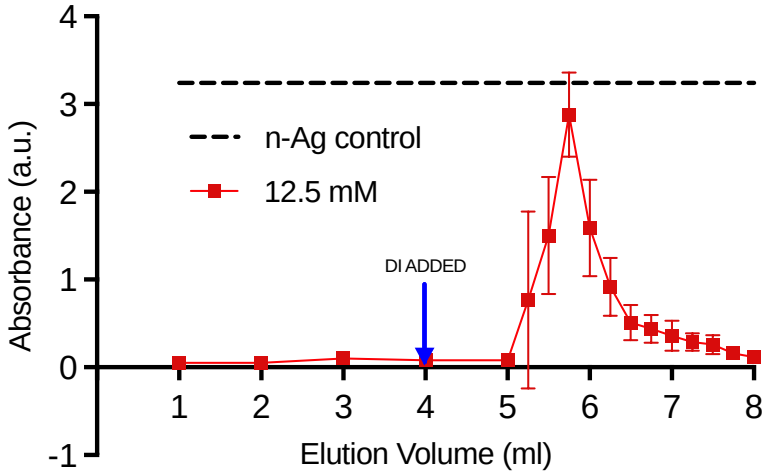

b)

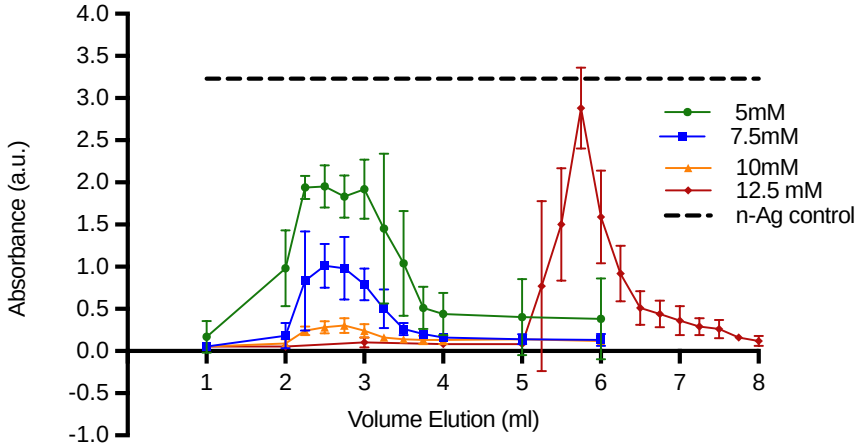

c)

Figure 2. Breakthrough curves at (a) 5 mM column elution (green line) and (b) 12.5 mM column elution (red line) represent the no capture and capture conditions. The blue arrow indicates when the Milli-Q water was added to the column. The dashed lines represent the pre-tested 0.05mg/ml nAg control samples. Between these ionic strengths (c) nAg elution at 7.5mM and 10mM.

3.2 UV-Visible Spectroscopy

The eluent UV-visible spectrophotometer absorbance was used to understand more about transport and retention conditions. The absorbance was tested for all the elution samples from the column. The initial absorbance of the nAg samples regardless of ionic strength was 3.23 ± 0.05 (nAg control). From mass balance and absorbance values the capture and transport of nAg at tested ionic strengths were heterogeneous. The maximum absorbance was 0.1 ± 0.06 in agreement with the absorbance of the pure 12.5 mM electrolyte solution (0.053 ± 0.002). The absorbance values for 12.5mM were consistent for all the effluent samples until Milli-Q water was added to the column, decreasing the ionic strength. The blue arrow indicates the introduction of Milli-Q water (figure 2 (b)). At 7.5mM and 10mM the capture and elution were partial with maximum absorbance values of 1.0 ± 0.3 and 0.3 ± 0.1 respectively.

3.3 DLVO Theory

ELECTROLYTE CONCENTRATION (mM)	DEBYE LENGTH (Å)	WELL DEPTH (kT)
5	43	-1.4 ± 0.2
7.5	35	-1.8
10	30	-2.2
12.5	27	-2.5

Table 2: Summary of Debye length and secondary minimum well depth for different electrolyte concentrations based on the DLVO calculation Eqs. 3 and 4.

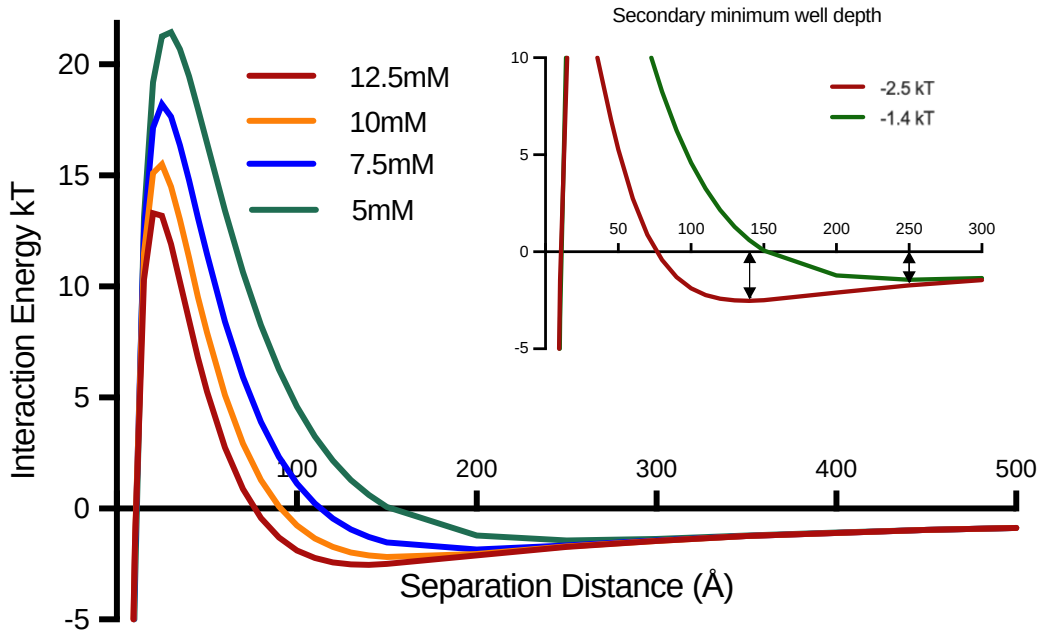

Figure 3. Interaction energy-distance profiles between nAg and SiO_2 from 5 to 12.5 mM. In the inset, the red line (12.5 mM) shows the well depth for capture is -2.5 kT and the green line (5 mM) shows no capture when the depth is decreased to about -1.5 kT. In between these extremes the behavior was mixed between elution and capture.

Based on the van der Waals attraction and electrostatic repulsion using the Poisson Boltzmann equation and constant surface potential, the total interaction energy was calculated at different salt concentrations (5, 7.5, 10, and 12.5 mM**)**. The secondary minimum depth values are summarized in Table 2. However, if the depth of the secondary minimum is shallow the colloidal particles could be eluted out due to Brownian motion (Shen et al.2012). The relevant range of ionic strength for the transition from no capture to retention ranges from 5 to 12.5 mM with mixed behaviors. Importantly, typical soil ionic strength is in 1 to 20 mM range (Cai et al. 2022). The energy differences across these ranges were approximately 1 kT (green compared to red lines in Figure 3), with varied behavior.

Because of the 3 orders of magnitude difference in the size of nAg and silica collector particles, the interaction is essentially independent of SiO_2 collector size and only depends on the nAg radius.

4. Conclusion

This work investigated the mobility of nAg at different ionic strengths in saturated porous media composed of micron-sized silica particles. The relevant range of ionic strength for monovalent salts to go from transport to capture was from 5mM to 12.5mM. The well-defined system enabled determination of the attractive well depth to capture nAg using DLVO theory. The captured nanoparticles were eluted upon decreasing the ionic strength and concomitant decrease in the depth of the secondary minimum. The results indicated that the behavior was heterogeneous for capture and elution of nAg for an ideal system with uniform silica collector particles .Surface roughness would likely change the depth of the secondary minimum well (Shen et al.2012).

Future work will drive towards more realistic systems by introducing dissolved organic matter (DOM), divalent salts, including roughness of collector particles, chemical heterogeneity as it may affect the retention of particles (Bradford and Torkzaban 2015; Shen et al.2012) and more complex soil mimics to better understand the transport and retention of nanoparticles in real systems.

5. References

1. Antonio Alves Júnior, J., & Baptista Baldo, J. (2014). The Behavior of Zeta Potential of Silica Suspensions. *New Journal of Glass and Ceramics*, *04*(02), 29–37. https://doi.org/10.4236/njgc.2014.42004
2. Badawy, A. M. E., Luxton, T. P., Silva, R. G., Scheckel, K. G., Suidan, M. T., & Tolaymat, T. M. (2010). Impact of Environmental Conditions (pH, Ionic Strength, and Electrolyte Type) on the Surface Charge and Aggregation of Silver Nanoparticles Suspensions. *Environmental Science & Technology*, *44*(4), 1260–1266. https://doi.org/10.1021/es902240k
3. Cai, W., Navarro, D. A., Du, J., Ying, G., Yang, B., McLaughlin, M. J., & Kookana, R. S. (2022). Increasing ionic strength and valency of cations enhance sorption through hydrophobic interactions of PFAS with soil surfaces. *Science of The Total Environment*, *817*, 152975. https://doi.org/10.1016/j.scitotenv.2022.152975
4. Cornelis, G., Pang, L., Doolette, C., Kirby, J. K., & McLaughlin, M. J. (2013). Transport of silver nanoparticles in saturated columns of natural soils. *Science of The Total Environment*, *463–464*, 120–130. https://doi.org/10.1016/j.scitotenv.2013.05.089
5. El Badawy, A. M., Aly Hassan, A., Scheckel, K. G., Suidan, M. T., & Tolaymat, T. M. (2013). Key Factors Controlling the Transport of Silver Nanoparticles in Porous Media. *Environmental Science & Technology*, *47*(9), 4039–4045. https://doi.org/10.1021/es304580r
6. Godinez, I. G., Darnault, C. J. G., Khodadoust, A. P., & Bogdan, D. (2013). Deposition and release kinetics of nano-TiO2 in saturated porous media: Effects of solution ionic

strength and surfactants. *Environmental Pollution*, *174*, 106–113. https://doi.org/10.1016/j.envpol.2012.11.002

7. Grabbe, A. (1993). Double-Layer Interactions Between Silylated Silica Surfaces. *Langmuir*, *9*(3), 797–801. https://doi.org/10.1021/la00027a032
8. Harvey, R. W., & Garabedian, S. P. (1991). Use of colloid filtration theory in modeling movement of bacteria through a contaminated sandy aquifer. *Environmental Science & Technology*, *25*(1), 178–185. https://doi.org/10.1021/es00013a021
9. Israelachvili, J. N. (1991). *Intermolecular and Surface Forces* (2nd ed.). Academic Press.
10. Israelachvili, J. N., & Adams, G. E. (1978). Measurement of forces between two mica surfaces in aqueous electrolyte solutions in the range 0–100 nm. *Journal of the Chemical Society, Faraday Transactions 1: Physical Chemistry in Condensed Phases*, *74*(0), 975. https://doi.org/10.1039/f19787400975
11. Lau, B. L. T., Hockaday, W. C., Ikuma, K., Furman, O., & Decho, A. W. (2013). A preliminary assessment of the interactions between the capping agents of silver nanoparticles and environmental organics. *Colloids and Surfaces A: Physicochemical and Engineering Aspects*, *435*, 22–27. https://doi.org/10.1016/j.colsurfa.2012.11.065
12. Lee, S. H., & Jun, B.-H. (2019). Silver Nanoparticles: Synthesis and Application for Nanomedicine. *International Journal of Molecular Sciences*, *20*(4), Article 4. https://doi.org/10.3390/ijms20040865
13. Liang, Y., Bradford, S. A., Simunek, J., Vereecken, H., & Klumpp, E. (2013). Sensitivity of the transport and retention of stabilized silver nanoparticles to physicochemical factors. *Water Research*, *47*(7), 2572–2582. https://doi.org/10.1016/j.watres.2013.02.025

14. Lin, S., Cheng, Y., Bobcombe, Y., L. Jones, K., Liu, J., & Wiesner, M. R. (2011). Deposition of Silver Nanoparticles in Geochemically Heterogeneous Porous Media: Predicting Affinity from Surface Composition Analysis. *Environmental Science & Technology*, *45*(12), 5209–5215. https://doi.org/10.1021/es2002327
15. Liu, Q., Sun, Z., & Santamarina, J. C. (2019). Transport and Adsorption of Silica Nanoparticles in Carbonate Reservoirs: A Sand Column Study. *Energy & Fuels*, *33*(5), 4009–4016. https://doi.org/10.1021/acs.energyfuels.9b00057
16. Mahdi, K. N. M., Peters, R., van der Ploeg, M., Ritsema, C., & Geissen, V. (2018). Tracking the Transport of Silver Nanoparticles in Soil: A Saturated Column Experiment. *Water, Air, & Soil Pollution*, *229*(10), 334. https://doi.org/10.1007/s11270-018-3985-9
17. Neukum, C., Braun, A., & Azzam, R. (2014). Transport of stabilized engineered silver (Ag) nanoparticles through porous sandstones. *Journal of Contaminant Hydrology*, *158*, 1–13. https://doi.org/10.1016/j.jconhyd.2013.12.002
18. Paramelle, D., Sadovoy, A., Gorelik, S., Free, P., Hobley, J., & Fernig, D. G. (2014). A rapid method to estimate the concentration of citrate capped silver nanoparticles from UV-visible light spectra. *Analyst*, *139*(19), 4855–4861. https://doi.org/10.1039/C4AN00978A
19. Patiño, J. E., Kuhl, T. L., & Morales, V. L. (2020). Direct Measurements of the Forces between Silver and Mica in Humic Substance-Rich Solutions. *Environmental Science & Technology*, *54*(23), 15076–15085. https://doi.org/10.1021/acs.est.0c05334
20. Sagee, O., Dror, I., & Berkowitz, B. (2012). Transport of silver nanoparticles (AgNPs) in soil. *Chemosphere*, *88*(5), 670–675. https://doi.org/10.1016/j.chemosphere.2012.03.055

21. Singh, S., Bharti, A., & Meena, V. K. (2014). Structural, thermal, zeta potential and electrical properties of disaccharide reduced silver nanoparticles. *Journal of Materials Science: Materials in Electronics*, *25*(9), 3747–3752. https://doi.org/10.1007/s10854-014-2085-x

22. *The Chemistry of Silica: Solubility, Polymerization, Colloid and Surface Properties and Biochemistry of Silica | Wiley*. (n.d.). Wiley.Com.

23. Tufenkji, N., & Elimelech, M. (2004). Correlation Equation for Predicting Single-Collector Efficiency in Physicochemical Filtration in Saturated Porous Media. *Environmental Science & Technology*, *38*(2), 529–536. https://doi.org/10.1021/es034049r

24. Wang, D., Ge, L., He, J., Zhang, W., Jaisi, D. P., & Zhou, D. (2014). Hyperexponential and nonmonotonic retention of polyvinylpyrrolidone-coated silver nanoparticles in an Ultisol. *Journal of Contaminant Hydrology*, *164*, 35–48. https://doi.org/10.1016/j.jconhyd.2014.05.007

25. Yao, K.-M., Habibian, M. T., & O'Melia, C. R. (1971). Water and waste water filtration. Concepts and applications. *Environmental Science & Technology*, *5*(11), 1105–1112. https://doi.org/10.1021/es60058a005

26. Lin, Shihong, Yingwen Cheng, Yohan Bobcombe, Kimberly L. Jones, Jie Liu, and Mark R. Wiesner. 2011. "Deposition of Silver Nanoparticles in Geochemically Heterogeneous Porous Media: Predicting Affinity from Surface Composition Analysis." *Environmental Science & Technology* 45(12):5209–15. doi: 10.1021/es2002327.

27. Bradford, Scott A., and Saeed Torkzaban. 2015. "Determining Parameters and Mechanisms of Colloid Retention and Release in Porous Media." *Langmuir* 31(44):12096–105. doi: 10.1021/acs.langmuir.5b03080

6. Supporting Information

Figure S1. Control measurements for UV-vis absorbance at 420 nm for 50 nm silver nanoparticles (nAg) as a function of concentration.
Figure S2. Size of nAg particles as a function of ionic strength measured by dynamic light scattering (DLS).

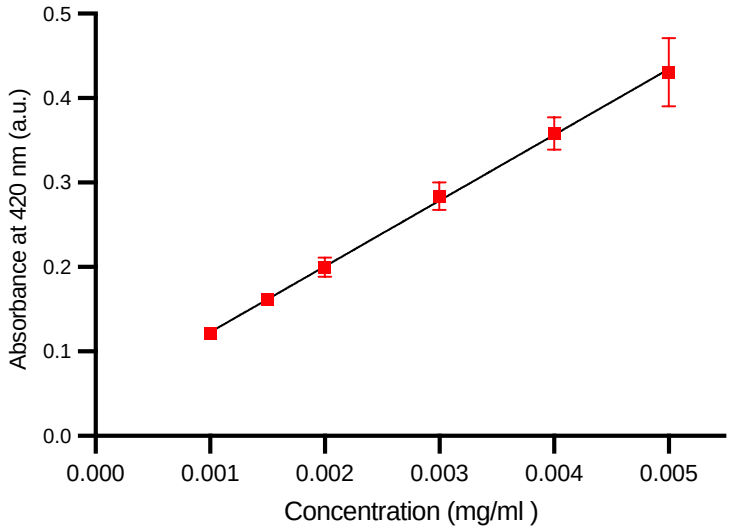

Figure S1. UV-vis calibration curve as a function of nAg concentration. Absorbance was measured at a wavelength of 420 nm.

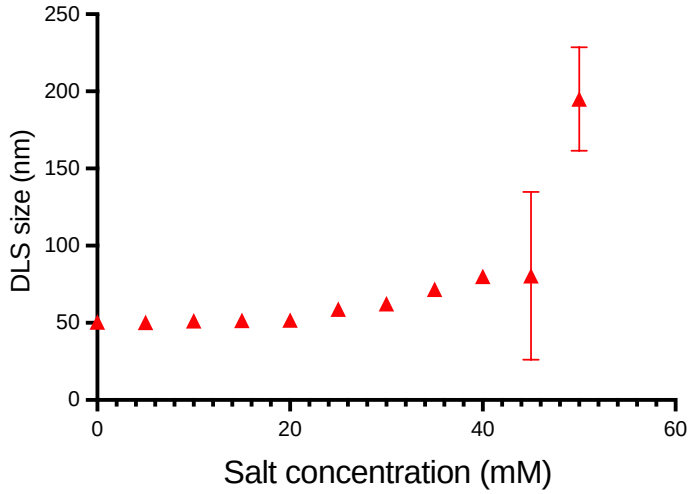

Figure S2. The size of nAg by dynamic light scattering (DLS) as a function of ionic strength in monovalent $NaNO_3$.

Reynolds number

Re =$\rho . v . L / \mu$

ρ- 1000 kg/m^3

Velocity

V = m *g / 6 Π r η

m = 4/3 Π r^3 ρ

ρ- density of silver -10.5 g/cm^3

m= 7 *10^{-19} kg

g =9.8 m/s^2

r = 25 *10^{-9}m

η- 1 *10^{-3} Ns/m^2

V = 1.5*10^{-8} m/s

Characteristic length - 0.125 m (length of column 12.5cm)

Dynamic viscosity - 1 *10^{-3} Ns/m^2

Re = 1.9 *10^{-5} (Laminar flow)

Peclet number

Pe =$L * v / D$

Velocity -1.5*10^{-8} m/s

Characteristic length - 0.125 m

Diffusivity of water =2.3 *10^{-9} m^2/s

Pe= 0.815 (Diffusive regime)

CONSERVATION OF MASS

The area under the curve was calculated using the Trapezoidal rule.

The total area under the curve for control = 3.23 ± 0.05 * 2ml = 6.46 (ml. a.u)

The mass recovery at 5mM - ~65%

7.5mM- ~ 24%

10mM- ~11%

12.5mM- ~8%

The total recovery with addition of DI in 12.5mM ~41%

All the mass recovery was calculated with cotton plug absorption of 16 ±13.5 %